Passive lossless snubbers for DC/DC converters

C.-L. Chen
C.-J. Tseng

Indexing terms: Passive lossless snubbers, Converters

Abstract: A general passive lossless snubber cell is proposed for use in DC/DC converters. The snubber is to suppress the turn-on loss of a MOSFET resulting from the reverse recovery current of the freewheeling diode. Energy recovery is achieved since the energy absorbed by the snubber during turn-on can be delivered to the output during turn-off. The simple structure and the absence of active components and resistors make this snubber a good alternative to a conventional RCD snubber or an active snubber. As an example, a boost converter equipped with the snubber is analysed. A 1kW, 100kHz prototype is implemented in the laboratory, and efficiency of 97% has been measured. Six basic non-isolated DC/DC converters equipped with the proposed snubber cell are also illustrated.

1 Introduction

Pulse width modulated (PWM) DC/DC converters have been widely used as switched mode power supplies in industry. The PWM technique is praised for its high power capability and ease of control. High power density and faster transient response of PWM DC/DC converters can be achieved by increasing the switching frequency. However, as the switching frequency increases, so do the switching losses and EMI noises. High switching losses reduce the power capabilities of PWM DC/DC converters, and serious EMI noises disturb control circuits.

Switching losses and EMI noises are mainly generated during turn-on and turn-off switching transitions of PWM DC/DC converters. According to Pietkiewicz and Tollik [1], there are three different non-ideal commutation phenomena behind this problem. The dominant phenomenon is the turn-on transient caused by the reverse recovery current of the freewheeling diode.

During the turn-on process of a MOSFET in a boost circuit, the reverse recovery phenomenon makes the diode conducting reversely discharge itself. The drain current contains input current and the reverse recovery current increases instantaneously, and full output voltage is applied between the drain and source because the diode is still conducting. Multiplication of the drain current and drain-source voltage during the turn-on transient causes serious thermal problems. Fast *di/dt* of the drain current also generates serious EMI noises.

Several kinds of snubbers heve been presented to reduce switching losses. Active snubbers [2] need auxiliary switches, and hence complex control strategies. RCD snubbers [3] dissipate power through the resistances, and thus reduce efficiency. A passive lossless snubber can effectively restrict switching losses by using no active and no power dissipative components. The circuit structure is simplified, and circuit efficiency is also effectively improved.

In this paper, a passive lossless snubber for boost PFC is investigated in depth. Snubber circuit operations are analysed, and component parameters can be mathematically determined. Experimental results from a 1kW, 100kHz boost PFC are used to verify the analysis. The general snubber cell for the boost converter is generalised to support the common non-isolated DC/DC converters.

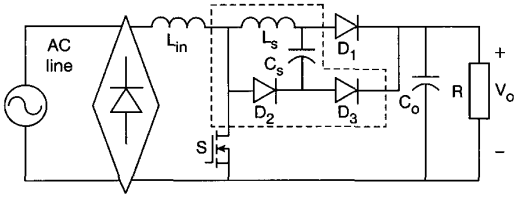

Fig. 1 *Boost converter with passive lossless snubber*

2 Boost PFC with a passive lossless snubber

2.1 Principle of operation

Fig. 1 shows a boost PFC with the studied snubber, which is encircled by dotted lines. During the turn-on process, diode D_1 conducts reversely to discharge itself. Growth rate of the reverse recovery current is restricted by the snubber inductor L_s, which is placed in series with diode D_1. After the reverse recovery of D_1, it is turned off and the first resonance path is formed by L_s, D_2 and C_s. The energy of L_s in current form is transferred to the snubber capacitor C_s in voltage form through diode D_2. After switch S turns off and the first resonance is stopped, the reverse recovery energy is delivered back to the output through the second resonance path V_s–L_{in}–L_s–C_s–D_3–V_o. This snubber absorbs the switching loss resulting from the reverse recovery current of diode D_1 and delivers it back to the output.

The circuit structure is simplified, and there are fewer components than with other energy recoverable snubbers.

IEE Proceedings online no. 19981877

Paper received 23rd April 1997

The authors are with the Power Electronics Laboratory, Department of Electrical Engineering, National Taiwan University, Taipei, Taiwan

2.2 Equivalent circuit analysis

To analyse the steady-state operations in one switching cycle of the circuit shown in Fig. 1, the following assumptions are made:

(i) the output capacitor C_o is large enough to assume that the output voltage V_o is constant and ripple-free.

(ii) input voltage V_s rectified from the AC voltage source is approximated to be constant in one switching cycle.

(iii) all semiconductor devices are assumed ideal, except the main diode D_1.

(iv) the input inductor L_{in} is much greater than the snubber inductor L_s.

In addition, the following six time steps are used:

t_0 = S turns on t_1 = D_1 is turned off t_2 = I_{Ls} becomes zero and D_2 is turned off

t_3 = S turns off D_2 and D_3 are turned on t_4 = D_2 is turned off

t_5 = V_{Cs} becomes zero, D_1 is turned on and D_3 is turned off

Two cases are analysed according to different duty ratios:

Case 1 (long duty) : t_0–t_1–t_2–t_3–t_4–t_5–t_0,

S turns off after I_{Ls} becomes zero.

Case 2 (short duty) : t_0–t_1–t_2–t_3–t_4–t_5–t_0,

S turns off before I_{Ls} becomes zero.

Based on these assumptions and classifications, the circuit operations of two cases in one switching cycle can be divided into six stages and are shown in Figs. 2–4, respectively.

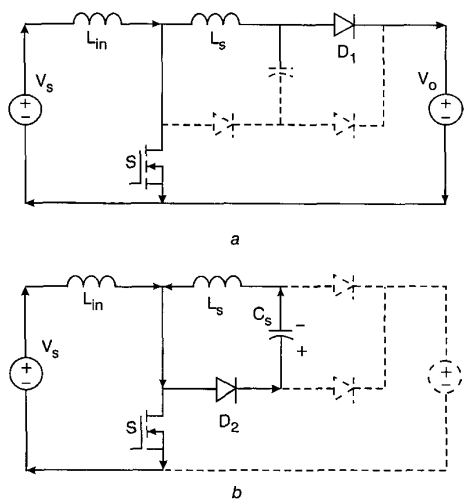

Fig.2 *Equivalent circuits during one switching cycle*
a Stage 1
b Stage 2

Stage 1 (Fig. 2*a*; $t_0 < t < t_1$)

Switch S turns on at t_0. The reverse recovery process makes diode D_1 conduct reversely to discharge itself. The inductor currents of L_{in} and L_s are given by

$$I_{Lin} = I_F(t_0) + \frac{V_s}{L_{in}}(t - t_0) \tag{1}$$

$$I_{Ls} = I_F(t_0) - \frac{V_o}{L_s}(t - t_0) \tag{2}$$

where $I_F(t_0)$ is the forward current through L_{in} and L_s at t_0.

Stage 2 (Fig. 2*b*; Case 1: $t_1 < t < t_2$, Case 2: $t_1 < t < t_3$)

The reverse recovery finishes and diode D_1 is off at t_1. Since D_1 is off, the reverse recovery current in L_s creates the first resonance path L_s–D_2–C_s to charge C_s through D_2. L_s and C_s create a one-way resonance because of diode D_2. The current through L_s and the voltage across C_s are given by

$$V_{Cs}(t) = \sqrt{\frac{L_s}{C_s}} I_{rr} \sin(\omega(t - t_1)) \tag{3}$$

$$I_{Ls}(t) = I_{rr} \cos(\omega(t - t_1)) \tag{4}$$

$$I_{rr} = -\left(I_F(t_0) - \frac{V_o}{L_s}(t - t_0)\right) \tag{5}$$

$$\omega = \frac{1}{\sqrt{L_s C_s}} \tag{6}$$

where I_{rr} is the peak value of the reverse recovery current through L_s and D_1. $0 < \omega(t - t_1) < \pi/2$ since diode D_2 makes L_s and C_s resonate in one direction.

Case 1 (long duty, $t_1 < t < t_2$): L_s and C_s stop resonating at t_2 before switch S turns off at t_3. Time t_2 is given by

$$t_2 = t_1 + \frac{\pi\sqrt{L_s C_s}}{2} \tag{7}$$

At t_2, I_{Ls} is equal to zero and V_{Cs} is given by

$$V_{Cs}(t_2) = \sqrt{\frac{L_s}{C_s}} I_{rr} \sin(\omega(t_2 - t_1)) = \sqrt{\frac{L_s}{C_s}} I_{rr} \tag{8}$$

Case 2 (short duty, $t_1 < t < t_3$): the duty is too short so that switch S turns off at t_3 before the resonance stops at t_2.

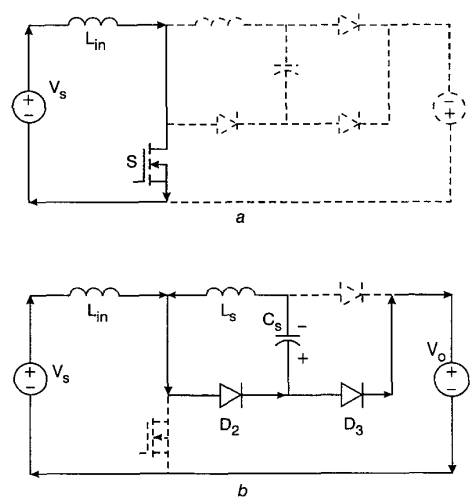

Fig.3 *Equivalent circuits during one switching cycle for stage 3*
a Case 1
b Case 2

Stage 3 (Fig. 3*a*, Case 1: $t_2 < t < t_3$; Fig. 3*b*, Case 2: $t_3 < t < t_2$)

Case 1 (long duty, $t_2 < t < t_3$): the current through L_s is zero and the voltage across C_s is constant after the first resonance is stopped by diode D_2 at t_2. The energy absorbed in L_s is completely delivered to C_s. Before switch S turns off at t_3, V_{Cs} is constant and I_{Ls} is zero, respectively.

Case 2 (short duty, $t_3 < t < t_2$): diode D_3 is turned on by the input inductor current $I_F(t_3)$ when switch S turns off at t_3. L_s and C_s keep resonating through the path L_s–D_2–C_s until the first resonance is stopped by diode D_2 at t_2. The input inductor current flows through diodes D_2 and D_3 to the output.

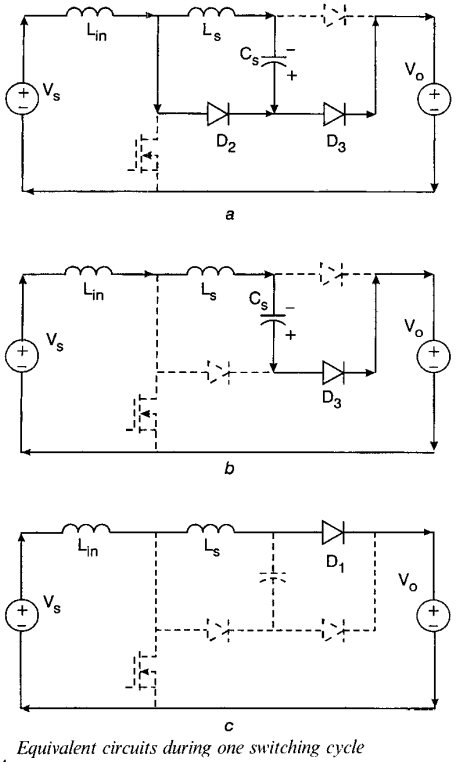

Fig. 4 *Equivalent circuits during one switching cycle*
a Stage 4
b Stage 5
c Stage 6

Stage 4 (Fig. 4*a*; Case 1: $t_3 < t < t_4$, Case 2: $t_2 < t < t_4$)

Case 1 (duty cycle is long, $t_3 < t < t_4$): diodes D_2 and D_3 are turned on by the input inductor current $I_F(t_3)$ when switch S turns off at t_3.

Case 2 (Duty cycle is short, $t_2 < t < t_4$): the first resonance is stopped and I_{Ls} is equal to zero at t_2. Time t_2 and the voltage V_{Cs} at t_2 are also given by eqns. 7 and 8, respectively.

Cases 1 and 2: since diode D_2 is on, the voltage across L_s is equal to V_{Cs} and makes I_{Ls} increase reversely to discharge C_s to the output. When I_{Ls} increases to the input inductor current $I_F(t_4)$ at t_4, diode D_2 is turned off automatically. Assuming that the input inductor current is constant at this stage, time t_4 when D_2 is automatically turned off and the voltage across C_s at t_4 are given by

$$t_4 = t_n + \sqrt{L_s C_s}\sin^{-1}\left(\frac{I_F(t_n)}{I_{rr}}\right) \tag{9}$$

$$V_{Cs}(t_4) = \sqrt{\frac{L_s}{C_s}(I_{rr}^2 - I_F(t_n)^2)} \tag{10}$$

where $t_n = t_3$ in Case 1 and $t_n = t_2$ in Case 2.

Stage 5 (Fig. 4*b*; $t_4 < t < t_5$)

The second resonance is formed by V_s–L_{in}–L_s–C_s–D_3–V_o when diode D_2 is turned off at t_4. In the second resonance, L_{in}, L_s and C_s are discharging to the output. All of the reverse recovery energy is completely transferred back to the output when V_{Cs} is discharged to zero through diode D_3 at t_5. Assuming that the input inductor current is constant at this stage, time t_5 when V_{Cs} becomes zero is given by

$$t_5 = t_4 + \frac{\sqrt{L_s C_s (I_{rr}^2 - I_F(t_4)^2)}}{I_F(t_4)} \tag{11}$$

Stage 6 (Fig. 4*c*; $t_5 < t < t_0$)

The energy recovery of the snubber finishes when diode D_1 is turned on at t_5. After that, the current $I_F(t_5)$ flows through diode D_1 instead of diode D_3 to prevent C_s from being charged reversely. Diode D_1 is turned on and D_3 is turned off at t_5. The input voltage source and the input inductor keep discharging to the output through diode D_1. The circuit operation is the same as in Stage 1 when switch S turns on again at t_0 in the next switching cycle.

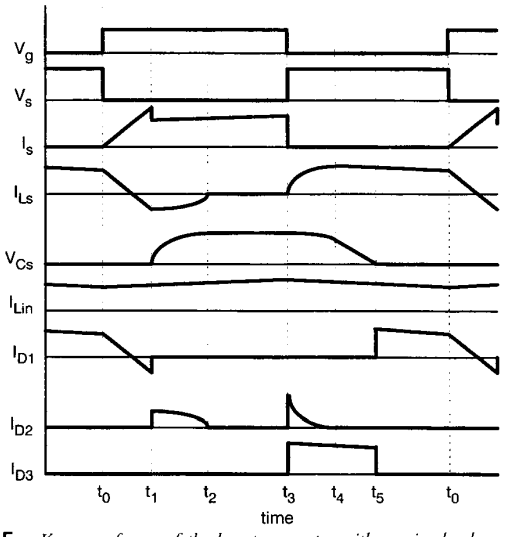

Fig. 5 *Key waveforms of the boost converter with passive lossless snubber for case 1 (long duty cycle long)*

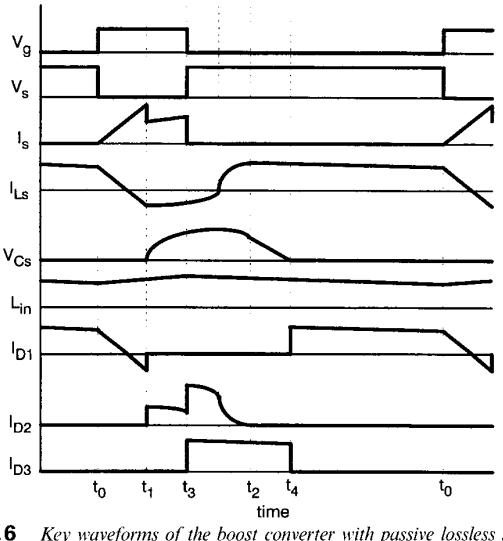

Fig. 6 *Key waveforms of the boost converter with passive lossless snubber for case 2 (short duty cycle)*

3 General snubber cell for DC/DC converters

The general passive lossless snubber cell is designed to suppress the turn-on switching loss resulting from the reverse recovery process of the freewheeling diode. It

follows that the proposed snubber can be generalised to support other basic DC/DC converters which suffer from the same switching loss. A general snubber cell is defined and shown in Fig. 7. Nodes A and K are connected to the anode and the cathode of the converter freewheeling diode D_1, respectively. Node A' is connected to the component that was connected to the anode of $D1$ in the original circuit.

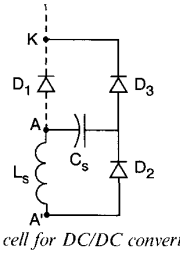

Fig. 7 *General snubber cell for DC/DC converter*

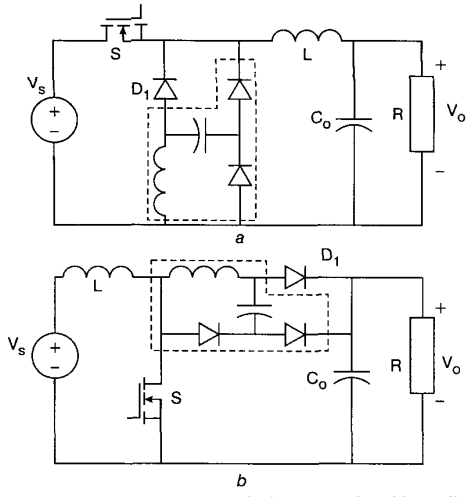

Fig. 8 *Basic DC/DC converters with the proposed snubber cells embedded*
a Buck converter with snubber
b Boost converter with snubber

The general snubber cell consists of one inductor L_s, one capacitor C_s and two diodes D_2 and D_3. The snubber inductor L_s is placed in series with the freewheeling diode D_1 to restrict the growth rate of the reverse recovery current when the switch turns on. After the turn-on transient, L_s, D_2 and C_5 form a resonance path to transfer the absorbed energy from L_s to C_s. Energy stored in C_s is delivered to the output through D_3 after the switch turns off. D_3 is turned off and D_1 is turned on after V_{Cs} is discharged to zero.

Snubber operation principles discussed in the boost converter example can be extended to other topologies. Six basic DC/DC converters are shown in Figs. 8–10 with the proposed snubber cells embedded.

4 Experimental results

4.1 Design example

The snubber inductor L_s and snubber capacitor C_s are the two main elements to be designed. In Stage 4, diode D_2 should be automatically turned off before the voltage of C_s is discharged to zero, or the residual current through D_2 will turn on D_2 and D_3 for the whole switching period. In other words, I_{rr} should be greater than I_F according to eqn. 9. Snubber inductor L_s should be as large as possible to decrease the reverse recovery loss, but I_{rr} should be kept larger than I_F. L_s can be determined by the following procedures.

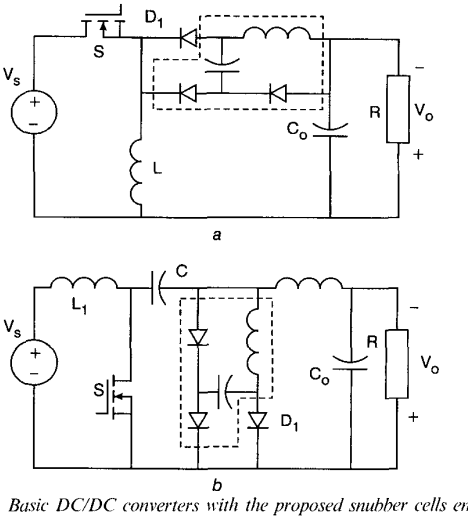

Fig. 9 *Basic DC/DC converters with the proposed snubber cells embedded*
a Buck-Boost converter with snubber
b Cuk converter with snubber

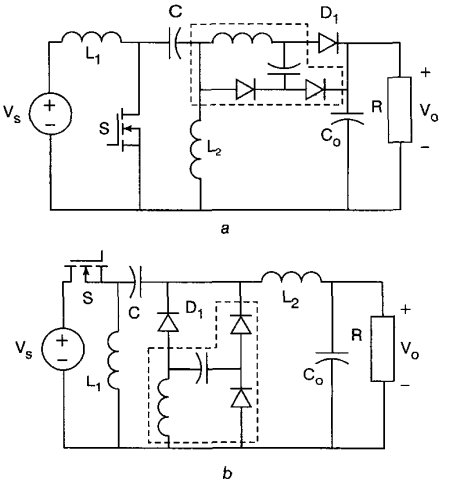

Fig. 10 *Basic DC/DC converters with the proposed snubber cells embedded*
a Sepic converter with snubber
b Zeta converter with snubber

Step 1: determine reverse recovery current peak value I_{rr}

The drain current of the MOSFET will have a transitional peak value equal to $I_F + I_{rr}$. I_{rr} can be determined by setting the peak value of the drain current and then subtracting I_F.

Step 2: calculate reverse current slope dI_R/dt

I_{rr} has the following relationship [4]:

$$I_{rr} \propto \sqrt{I_F \frac{dI_R}{dt}} \tag{12}$$

I_{rr} for specified I_F and dI_R/dt can be found in a data book. The reverse current slope dI_R/dt can be obtained by using I_F and I_{rr} calculated in Step 1 in eqn. 12.

Step 3: determine snubber inductor L_s

The equation $V = L_s(dI_R/dt)$ is used to determine L_s, where V is the output voltage and I_R is the current through D_1 as well as L_s. L_s can be determined by

$$L_s = \frac{V}{\frac{dI_R}{dt}} \tag{13}$$

The voltage rating of D_1 is equal to the output voltage plus V_{Cs}. The snubber capacitor C_s should be as small as possible to reduce the resonant period and to prevent an excessively high voltage rating of D_1. The recommended value of V_{Cs} is 50 ~ 100V and C_s can be determined by eqn. 8.

Table 1: Part list of the implemented prototype power circuit

Part	Type	Part	Value
S	IRFP460	L_s	2μH
D_1	HFA15TB60	C_s	100nF
D_2	HFA15TB60	L	180μH
D_3	HFA15TB60	C	940μF

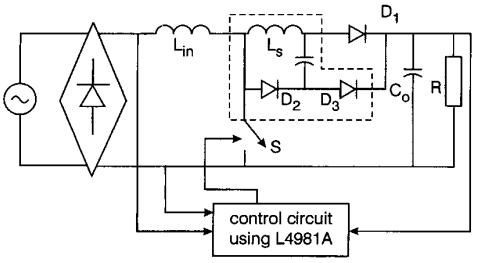

Fig. 11 *Simplified circuit of implemented prototype*

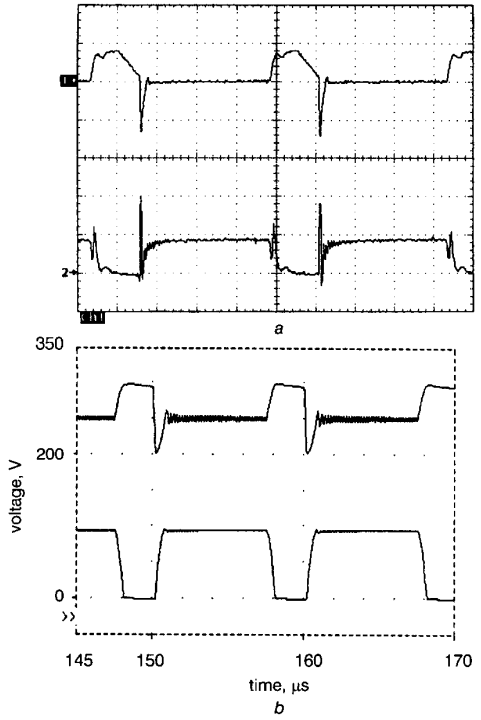

Fig. 12 *Waveforms of snubber inductor current and snubber capacitor voltage*
a Experimental results
b Simulation results

4.2 Experimental waveforms

To experimentally verify the principle of operation and the theoretical analysis, a prototype of 1kW, 100kHz boost converter with the passive lossless snubber is implemented. Control strategy is implemented with a L4981A. This prototype is regulated at 400V DC output with 220V AC input. A simplified circuit of the implemented prototype is shown in Fig. 11, with the components specifications listed in Table 1.

The snubber inductor current and snubber capacitor voltage waveforms are shown in Fig. 12*a*, and PSPICE simulation results are shown in Fig. 12*b*. The waveforms in Fig. 12 can be collated with those of V_{Cs} and I_{Ls} in Fig. 6*a*.

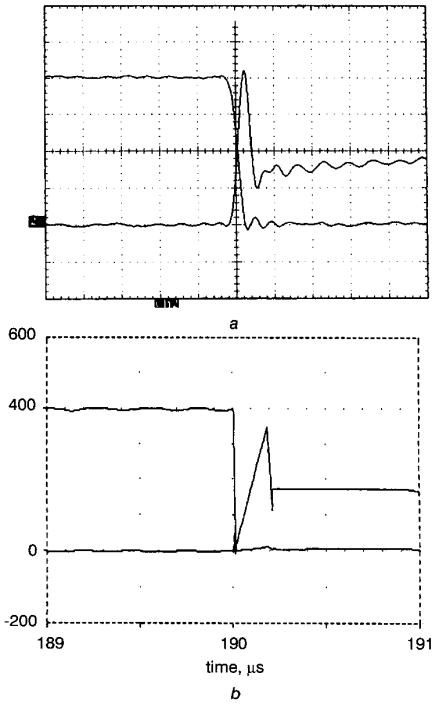

Fig. 13 *Waveforms of MOSFET commutation with the proposed snubber*
a Experimental results
b Simulation results

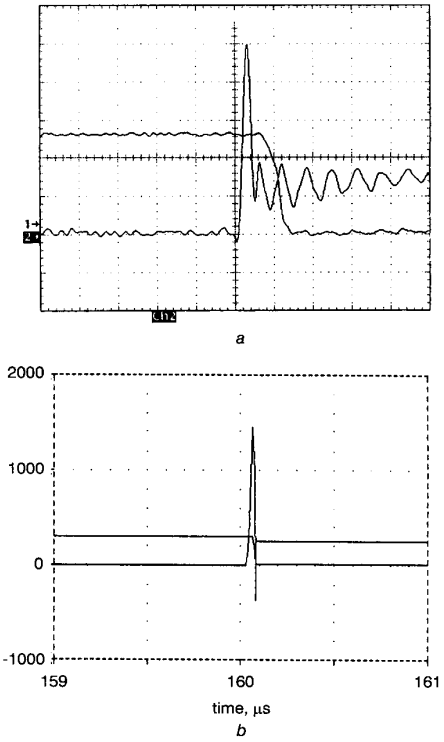

Fig. 14 *Waveforms of MOSFET commutation without snubber*
a Experimental results
b Simulation results

The commutation waveforms of the MOSFET with the proposed snubber are shown in Fig. 13*a*, and PSPICE simulation results are shown in Fig. 13*b*. Counterparts without the snubber are shown in Fig. 14*a* and *b*, respectively, to contrast with Fig. 13. It is easily seen that the turn-on loss is apparently reduced and the MOSFET commutates near the ZCS (zero-current-switch). The reason for the ZCS is the discharge of the parasitic drain-source capacitance of the MOSFET during the turn-on process. This switching loss can only be removed by resonant converter techniques or active snubbers. It can also be seen that the growth rate of the drain current is effectively eliminated. EMI noises are reduced due to the slower *di/dt* of drain current. Efficiency of 97% at 1kW loading has been measured by the Voltech PM3000A.

5 Conclusion

A general passive lossless snubber cell for DC/DC converters has been proposed. The general snubber cell is composed of only one inductor, one capacitor and two diodes. The cell is designed to suppress turn-on switching losses caused by the reverse recovery current of the freewheeling diode. Steady-state circuit operations of a boost circuit with the proposed snubber have been analysed. Experimental waveforms of the MOSFET commutation show that the snubber can effectively suppress the reverse recovery loss and eliminate the *di/dt* of the drain current. The snubber inductor and capacitor for the boost topology can be precisely determined by the presented design. The circuit operation analysis and design rules are also valid when applying the snubber to other topologies.

6 References

1 PIETKIEWICZ, A., and TOLLIK, D.: 'Snubber circuit and Mosfet paralleling considerations for high power boost-based power-factor correctors'. INTELEC '95, pp. 41–45

2 LIN, R.L., and LEE, F.C.: 'Novel zero-current-switching-zero-voltage-switching converters'. PESC '96, pp. 438–442

3 FINNEY, S.J., WILLIAMS, B.W., and GREEN, T.C.: 'The RCD snubber revisited'. IAS '93, pp. 1267–1273

4 MOHAN, N., UNDELAND, T., and ROBBINS, W.: 'Power electronics: converters, applications and design' (Wiley, 1989), pp. 462–467